

Cite this: *Chem. Commun.*, 2011, **47**, 11703–11705

www.rsc.org/chemcomm

COMMUNICATION

A robust pure hydrocarbon derivative based on the (2,1-*b*)-indenofluorenyl core with high triplet energy level†Cyril Poriel,^{*a} Rémi Métivier,^b Joëlle Rault-Berthelot,^a Damien Thirion,^a Frédéric Barrière^a and Olivier Jeannin^a

Received 25th July 2011, Accepted 8th September 2011

DOI: 10.1039/c1cc14534g

A unique (2,1-*b*)-indenofluorenyl core flanked with two spirofluorene units, possessing a high triplet energy value and excellent thermal/morphological stability, is reported.

Phenylene derivatives constitute an important class of molecules, which have been widely studied in the last decade due to their potential applications in organic electronics.¹ Of particular interest in oligophenylene chemistry and physics is the (1,2-*b*)-indenofluorenyl core, which is nowadays an important building block for blue fluorescent organic light emitting diodes (OLEDs),^{1–7} organic field effect transistors,^{8,9} organic solar cells,¹⁰ and for green phosphorescent OLEDs (PhOLEDs).¹¹ More recently the (2,1-*a*)-indenofluorenyl core, a positional isomer of the (1,2-*b*)-indenofluorenyl core, has also been investigated for potential organic electronics applications^{12–15} and has emerged as an appealing scaffold for the modulation of optical properties of dispirofluorene-indenofluorene derivatives.^{13–15} Due to the importance of the (1,2-*b*)- and (2,1-*a*)-indenofluorenyl cores in organic electronics, it hence appears of great interest to design other indenofluorene isomers, which might be used in optoelectronics. For example, the design of organic host materials for blue phosphorescent emitters possessing a very high triplet energy value ($E_T > 2.7$ eV)^{16,17} represents a highly challenging task for the future of organic electronics. Of particular interest for this technology are pure hydrocarbon derivatives, which have been very rarely used as host materials for blue PhOLED applications due to the difficulty in achieving high E_T , keeping intact the other physical properties (good carrier transporting, thermal and morphological properties).^{18–20} There is indeed a trade-off between increasing the HOMO–LUMO gap of a pure hydrocarbon molecule to increase the singlet and triplet level energy values and decreasing the conjugation length of the π -aromatic backbone, which may adversely affect the thermal and morphological stability. In our quest for robust pure

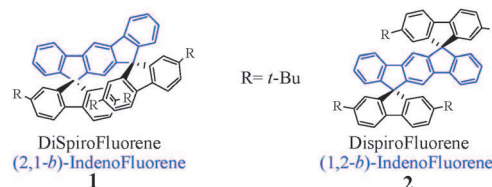


Fig. 1 (2,1-*b*)-DSF(*t*-Bu)₄-IF **1** and its positional isomer (1,2-*b*)-DSF(*t*-Bu)₄-IF **2**.

hydrocarbon derivatives with very high E_T , we report herein a unique molecular design based on a *meta*-substituted terphenylene core, namely (2,1-*b*)-indenofluorene, flanked with two spirofluorene units ((2,1-*b*)-DSF(*t*-Bu)₄-IF **1**, Fig. 1). This molecular design should in principle lead to high E_T due to the (2,1-*b*)-indenofluorenyl core, keeping however excellent morphological and thermal properties thanks to the two spirofluorene units.²¹ This work is to the best of our knowledge the first example of a (2,1-*b*)-indenofluorenyl core and one of the highest E_T ever reported for pure hydrocarbon derivatives of interest for organic electronics.^{18–20,22}

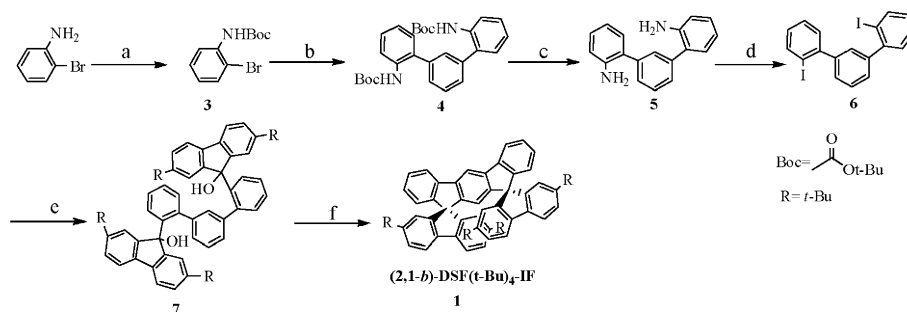
Geometry optimization of **1** and **2** in the singlet and triplet states was performed using density functional theory at the Gaussian03 B3LYP/6-31G* level, followed by a single point calculation on the optimized structures using B3LYP/6-311+G**. The calculated energies of the frontier molecular orbitals (and the corresponding HOMO–LUMO gap) are, respectively, –5.61 and –1.32 eV ($\Delta E = 4.29$ eV) for **1** and –5.59 and –1.52 eV ($\Delta E = 4.07$ eV) for **2**. The computed triplet adiabatic S_0 to T_1 excitation energy,^{23,24} defined as the energy difference between the highest occupied molecular orbitals in the relaxed geometry of the molecules in their singlet and triplet states, is 2.69 eV for **1** and 2.53 eV for **2**. Thus, **1** is expected to have higher E_T than that of its related positional isomer **2**.

The first step of our synthetic investigations (Scheme 1) towards the synthesis of **1** was to protect the amino group of the starting material, 1-bromoaniline, with a *tert*-butylcarbamoyl (Boc) group. The use of the non-nucleophilic strong base sodium hexamethyldisilazane (NaHMDS) prior to the addition of the di-*tert*-butyldicarbonate (Boc₂O) gave the corresponding *tert*-butyl-carbamoylated derivative **3**. Reaction of **3** with 1,3-phenylenebisboronic acid under Suzuki–Miyaura cross-coupling conditions using [Pd^{II}Cl₂(dppf)]·CH₂Cl₂ as the catalyst led to the terphenyl **4** in high yield (87%). Deprotection of the amino

^a Université de Rennes 1, UMR CNRS 6226, Campus de Beaulieu, 35042 Rennes cedex, France. E-mail: cyril.poriel@univ-rennes1.fr

^b PPSM, ENS Cachan, UMR CNRS 8531, 61 Avenue du Président Wilson, 94235 Cachan, France

† Electronic supplementary information (ESI) available: Synthetic procedures, complete compounds characterizations, thermal, optical and electrochemical data and copy of NMR spectra. CCDC 836979. For ESI and crystallographic data in CIF or other electronic format see DOI: 10.1039/c1cc14534g



Scheme 1 Synthesis of **1**: (a) 1. NaHMDS, THF, rt; 2. Boc₂O; (76%) (b) 1,3-C₆H₄(B(OH)₂)₂, [Pd^{II}Cl₂(dppf)]·CH₂Cl₂, Na₂CO₃, DMF/H₂O, 90 °C (87%); (c) TFA, CH₂Cl₂, 0 °C → rt (99%); (d) 1. NaNO₂, H₂O/HCl, 0 °C; 2. KI/H₂O, 0 °C → 60 °C (53%). (e) 1. *n*-BuLi/THF, −78 °C 2. 2,7-*tert*-butyl-fluoren-9-one, −78 °C → rt (20%); (f) BF₃·OEt₂/CH₂Cl₂, rt (85%).

groups was then performed under acidic conditions and the diamino derivative **5** was quantitatively obtained. Using a 10-fold excess of KI as described by Holmes and co-workers,²⁵ key compound **6** was finally obtained through a Sandmeyer reaction in 53% yield. Lithium–iodine exchange of **6** with *n*-butyllithium followed by the addition of 2,7-*tert*-butyl-fluoren-9-one²⁶ afforded the corresponding difluorenol **7** (20%), which was further cyclized through an intramolecular electrophilic bicyclization reaction to afford the target (2,1-*b*)-DSF(*t*-Bu)₄-IF **1** with the (2,1-*b*)-indenofluorenyl core. We note that compound **6** reported herein widens the scope of diiodinated terphenyl isomers as key building blocks for the synthesis of spiro derivatives for organics electronics.^{21,27}

The structure of **1** has been confirmed by X-ray diffraction on single crystals obtained by slow diffusion of pentane in a THF solution (Fig. 2).[†] The (2,1-*b*)-indenofluorenyl core has a maximum length of 10.7 Å, shorter than their positional isomers (1,2-*b*- or (2,1-*a*)-indenofluorenyl cores (respectively 11.1 Å and 10.8 Å).²⁶ This contraction of the (2,1-*b*)-indenofluorenyl core is caused by its “crescent moon” shape due to the *meta*-linkages of the constituting phenylene rings. The (2,1-*b*)-indenofluorenyl core is almost flat with dihedral angles between the plane of the central phenyl ring and those of the side rings of *ca.* 3.9° and 0.7°. In addition, the distance between the two spiro carbons is *ca.* 5.2 Å and the two fluorenyl units display an eclipsed conformation. These two features clearly indicate that the two face-to-face fluorene units are too far from one another to allow intramolecular π -stacking interactions.[§]

The electrochemical oxidation of **1**, investigated by cyclic voltammetry and differential pulse voltammetry, consists of two successive isoelectronic reversible oxidations with maxima at 1.44 and 1.62 V, respectively, followed by a third multi-electronic oxidation at 1.94 V (see ESI[†]). Multiple scans including the three waves lead to the deposition of an insoluble electroactive film on the electrode surface due to anodic polymerization processes.⁶ From the onset oxidation potential,²⁸ we determined the HOMO level of **1** lying at −5.73 eV, slightly

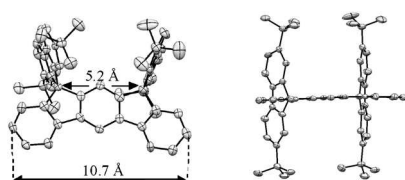


Fig. 2 ORTEP drawing of **1** (ellipsoid probability at 50% level, hydrogen atoms have been omitted for clarity).

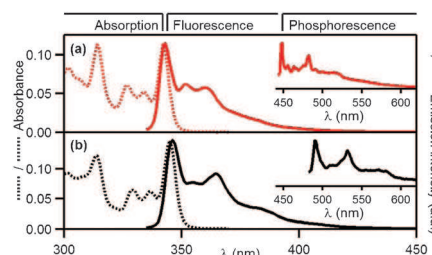


Fig. 3 Absorption (dotted line) and fluorescence emission (solid line, $\lambda_{\text{exc}} = 330$ nm) spectra of **1** (a) and **2** (b) in methylcyclohexane/2-methylpentane 1 : 1 at rt. Insets: phosphorescence spectra at 77 K.

below that of its isomer **2** (HOMO: −5.61 eV).²⁶ As the cyclic voltammeteries recorded in the cathodic range do not show any well-defined reduction wave allowing an accurate electrochemical band gap measurement (see ESI[†]), the LUMO of **1** (−2.19 eV) was determined from the optical band gap and the HOMO level.

The UV-Vis absorption spectrum of **1** in methylcyclohexane/2-methylpentane 1 : 1 exhibits five characteristic absorption bands (302, 314, 327, 334, 342 nm), very similar to those previously observed for its positional isomer **2** with however, a slight blue shift (3 nm) between the two maxima (342 nm for **1** vs. 345 nm for **2**), Fig. 3. The optical band gaps of **1** and **2** are, respectively, 3.55 eV and 3.52 eV. The slight band gap contraction observed in **2** coupled to its higher HOMO level (*vide supra*) suggests a better delocalization of π -electrons in **2** compared to **1**. Similarly, the fluorescence spectrum of **1** (Fig. 3a), with a maximum recorded at 343 nm, is also blue-shifted compared to **2** ($\lambda_{\text{max}} = 346$ nm, Fig. 3b). The fluorescence spectral shape of **1** is the mirror image of its absorption spectrum and the Stokes shift is almost negligible, indicating very little rearrangements in the excited state and hence a highly rigid structure. The fluorescence quantum yield of **1** was measured to be 0.51 and a fluorescence lifetime of 3.85 ns (in THF) was determined, showing that **1** is a very efficient blue-violet fluorescent emitter.

At 77 K, in a frozen methylcyclohexane/2-methylpentane 1 : 1 glassy matrix, the phosphorescence spectra of both isomers were recorded: $\lambda_{\text{max}} = 448$ and 482 nm for **1** and $\lambda_{\text{max}} = 490$ and 532 nm for **2**. Deactivation of the triplet state of compounds **1** and **2** is very slow under these experimental conditions: the phosphorescence decay was measured and the lifetime of the T₁ state of **1** (resp. **2**) was found to be 4.8 s (resp. 2.9 s), in accordance with data reported for closely related compounds.²⁹ The corresponding E_{T} values of **1** and **2** obtained by the highest-energy

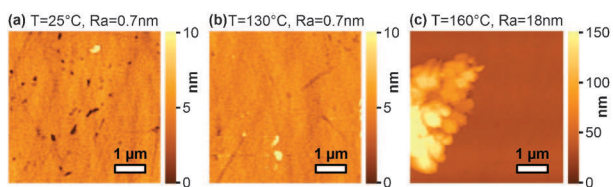


Fig. 4 AC-AFM images of a vacuum-deposited thin-film of **1** ($5 \times 5 \mu\text{m}$): non-heated film (a). Film heated (1 h) in air at 130 °C (b) and 160 °C (c).

phosphorescent peak were thus, respectively, estimated at *ca.* 2.76 eV and 2.52 eV. The *meta*-substituted terphenyl backbone found in **1** leads hence to a remarkable increase of the E_T value compared to the *para*-substituted terphenyl backbone found in **2**. Thus, the E_T value of **2** appears to be higher than the E_T value of Ir(ppy)₃ ($E_T = 2.42$ eV),¹⁶ an efficient green phosphorescent emitter, and the E_T value of **1** appears to be higher than the E_T value of Flrpic ($E_T = 2.64$ eV),¹⁶ an efficient blue phosphorescent emitter.

Finally, the morphology of vacuum deposited thin-films of **1** on quartz slides has been studied by atomic force microscopy in acoustic mode (AC-AFM) in order to evaluate the effect of temperature and ambient atmosphere on the thin-film structure. The surface has been exposed to air under thermal stress conditions from room temperature to 200 °C (Fig. 4 and figures in ESI†). The non-heated film surface presents a regular and smooth morphology (Fig. 4a). The surface roughness (R_a) of the film appears to be very low, around 0.7 nm, and is kept almost unchanged until 130 °C (Fig. 4b), highlighting the very good quality of the film surface and the high stability of **1** upon heating. At 160 °C, the surface morphology became however rough with R_a estimated around 18 nm, likely caused by degradation and/or crystallization of the material (Fig. 4c).^{30–32} **1** presents hence an excellent morphological stability under very harsh conditions and this stability up to 130 °C under an ambient atmosphere is a key point before any possible OLED applications. Thermogravimetric analysis (see ESI†) confirms the excellent thermal stability of **1** with a decomposition temperature²¹ T_d of 387 °C, even higher than that of its isomer **2** ($T_d = 350$ °C).²⁶

To summarize, we have designed and synthesized through an efficient synthetic approach (2,1-*b*)-DSF(*t*-Bu)₄-IF **1** containing the novel (2,1-*b*)-indenofluorenyl spirolinked to two fluorenyl units. This simple molecular concept allows us to combine within a single pure hydrocarbon molecule a high E_T with a very long phosphorescence lifetime and excellent thermal and morphological stability. This work is the first example of a (2,1-*b*)-indenofluorenyl core and one of the highest E_T ever reported for a morphologically stable pure hydrocarbon derivative of interest for organic electronics.

We wish to thank the CDIFX, the C.R.M.P.O (Rennes) and the CINES (Montpellier). We also thank A. Brosseau (Cachan), Dr J. F. Bergamini (Rennes) for AFM images, F. Moreau (Rennes) for the TGA and the Région Bretagne for a studentship (DT).

Notes and references

† Selected data for **1**: C₆₅H₇₀, $M = 851.21$, triclinic, space group *P*-1, $a = 11.383(3)$ Å, $b = 12.212(3)$ Å, $c = 19.173(5)$ Å, $\alpha = 84.385(6)^\circ$, $\beta = 88.389(11)^\circ$, $\gamma = 70.418(6)^\circ$, $V = 2494.3(13)$ Å³, $Z = 2$, $T = 150$ K,

Mo-K α ($\lambda = 0.71073$ Å) $D_c = 1.133$ g cm⁻³, $\mu(\text{Mo}) = 0.063$ mm⁻¹, 15 549 reflections measured, of which 8656 independent ($R_{\text{int}} = 0.0738$), $R_f = 0.1044$ [4180 data, $I > 2\sigma(I)$], $wR(F^2) = 0.3389$, GOF = 1.056.

§ For structural features related to other dispirofluorene-indenofluorenes with interacting face-to-face fluorene units, see ref. 13–15.

- 1 A. C. Grimsdale and K. Müllen, *Macromol. Rapid Commun.*, 2007, **28**, 1676–1702.
- 2 Z. Ma, P. Sonar and Z.-K. Chen, *Curr. Org. Chem.*, 2010, **18**, 2039–2069.
- 3 A. C. Grimsdale, K. L. Chan, R. E. Martin, P. G. Jokisz and A. B. Holmes, *Chem. Rev.*, 2009, **109**, 897–1091.
- 4 J. Jacob, J. Zhang, A. C. Grimsdale, K. Müllen, M. Gaal and E. J. W. List, *Macromolecules*, 2003, **36**, 8240–8245.
- 5 D. Marsitzky, J. C. Scott, J.-P. Chen, V. Y. Lee, R. D. Miller, S. Setayesh and K. Müllen, *Adv. Mater.*, 2001, **13**, 1096–1099.
- 6 (a) N. Cocherel, C. Poriol, L. Vignau, J.-F. Bergamini and J. Rault-Berthelot, *Org. Lett.*, 2010, **12**, 452–455; (b) D. Thirion, J. Rault-Berthelot, L. Vignau and C. Poriol, *Org. Lett.*, 2011, **13**, 4418–4421.
- 7 Y. Park, J.-H. Lee, D. H. Jung, S.-H. Liu, Y.-H. Lin, L.-Y. Chen, C.-C. Wu and J. Park, *J. Mater. Chem.*, 2010, **20**, 5930–5936.
- 8 W. Zhang, J. Smith, R. Hamilton, M. Heeney, J. Kirkpatrick, K. Song, S. E. Watkins, T. Anthopoulos and I. McCulloch, *J. Am. Chem. Soc.*, 2009, **131**, 10814–10815.
- 9 H. Usta, C. Risko, Z. Wang, H. Huang, M. K. Delimeroglu, A. Zhukhovitskiy, A. Facchetti and T. J. Marks, *J. Am. Chem. Soc.*, 2009, **131**, 5586–5608.
- 10 J. Kim, S. H. Kim, I. H. Jung, E. Jeong, Y. Xia, S. Cho, I.-W. Hwang, K. Lee, H. Suh, H.-K. Shim and H. Y. Woo, *J. Mater. Chem.*, 2010, **20**, 1577–1586.
- 11 L.-C. Chi, W.-Y. Hung, H.-C. Chiu and K.-T. Wong, *Chem. Commun.*, 2009, 3892–3894.
- 12 Covion Organic Semiconductors: Eur. Pat. Appl., EP 1491568, 2004.
- 13 D. Thirion, C. Poriol, J. Rault-Berthelot, F. Barrière and O. Jeannin, *Chem.–Eur. J.*, 2010, **16**, 13646–13658.
- 14 D. Thirion, C. Poriol, F. Barrière, O. Jeannin, R. Métivier and J. Rault-Berthelot, *Org. Lett.*, 2009, **11**, 4794–4797.
- 15 D. Thirion, C. Poriol, R. Métivier, J. Rault-Berthelot, F. Barrière and O. Jeannin, *Chem.–Eur. J.*, 2011, **17**, 10272–10287.
- 16 H. Yersin, *Highly Efficient OLEDs with Phosphorescent Materials*, Wiley-VCH: Verlag GmbH & Co. KGaA, Weinheim, 2007.
- 17 L. Xiao, Z. Chen, B. Qu, J. Luo, S. Kong, Q. Gong and J. Kido, *Adv. Mater.*, 2011, **23**, 926–952.
- 18 Y. Tao, C. Yang and J. Qin, *Chem. Soc. Rev.*, 2011, **40**, 2943–2970.
- 19 C. Fan, Y. Chen, P. Gan, C. Yang, C. Zhong, J. Qin and D. Ma, *Org. Lett.*, 2010, **12**, 5648–5651.
- 20 S. Ye, Y. Liu, C.-a. Di, H. Xi, W. Wu, Y. Wen, K. Lu, C. Du, Y. Liu and G. Yu, *Chem. Mater.*, 2009, **21**, 1333–1342.
- 21 T. P. I. Saragi, T. Spehr, A. Siebert, T. Fuhrmann-Lieker and J. Salbeck, *Chem. Rev.*, 2007, **107**, 1011–1065.
- 22 Z. Jiang, H. Yao, Z. Zhang, C. Yang, Z. Liu, Y. Tao, J. Qin and D. Ma, *Org. Lett.*, 2009, **11**, 2607–2610.
- 23 P. Marsal, I. Avilov, D. A. da Silva Filho, J. L. Bredas and D. Beljonne, *Chem. Phys. Lett.*, 2004, **392**, 521–528.
- 24 H. Sasabe, Y.-J. Pu, K.-I. Nakayama and J. Kido, *Chem. Commun.*, 2009, 6655–6657.
- 25 K. L. Chan, M. J. McKiernan, C. R. Towns and A. B. Holmes, *J. Am. Chem. Soc.*, 2005, **127**, 7662–7663.
- 26 C. Poriol, J. Rault-Berthelot, F. Barrière and A. M. Z. Slawin, *Org. Lett.*, 2008, **10**, 373–376.
- 27 D. Horhant, J.-J. Liang, M. Virboul, C. Poriol, G. Alcaraz and J. Rault-Berthelot, *Org. Lett.*, 2006, **8**, 257–260.
- 28 A. P. Kulkarni, C. J. Tonzola, A. Babel and S. A. Jenekhe, *Chem. Mater.*, 2004, **16**, 4556–4573.
- 29 D. Hertel, S. Setayesh, H. G. Nothofer, U. Scherf, K. Müllen and H. Bässler, *Adv. Mater.*, 2001, **13**, 65–70.
- 30 S. Liu, F. He, H. Wang, H. Xu, C. Wang, F. Li and Y. Ma, *J. Mater. Chem.*, 2008, **18**, 4802–4807.
- 31 S.-K. Kim, Y.-I. Park, I.-N. Kang and J.-W. Park, *J. Mater. Chem.*, 2007, **17**, 4670–4678.
- 32 C.-H. Wu, C.-H. Chien, F.-M. Hsu, P.-I. Shih and C.-F. Shu, *J. Mater. Chem.*, 2009, **19**, 1464–1470.